Chemical Engineering Science 94 (2013) 245–255

Contents lists available at SciVerse ScienceDirect

Chemical Engineering Science

journal homepage: www.elsevier.com/locate/ces

Nonstandard finite difference schemes based on Green's function formulations for reaction–diffusion–convection systems

Eliseo Hernandez-Martinez [a,*], Hector Puebla [b], Francisco Valdes-Parada [c], Jose Alvarez-Ramirez [c]

[a] Matemáticas Aplicadas y Computación, Instituto Mexicano del Petróleo, D.F., Mexico
[b] Departamento de Energía, Universidad Autónoma Metropolitana-Azcapotzalco, D.F., Mexico
[c] Departamento de IPH, Universidad Autonoma Metropolitana-Iztapalapa, D.F., Mexico

HIGHLIGHTS

- Numerical solutions of RDC systems are given using an integral formulation approach.
- Nonstandard finite differences are a particular case of integral formulations.
- The scheme proposed exhibit global approximation orders of $O(h^2)$.
- Proposed scheme exhibit better numerical approximation than traditional schemes.

ARTICLE INFO

Article history:
Received 4 October 2012
Received in revised form
19 February 2013
Accepted 1 March 2013
Available online 13 March 2013

Keywords:
Nonstandard finite differences
Green's functions
Transport processes
Chemical processes
Dynamic simulation
Numerical analysis

ABSTRACT

Nonstandard finite differences (NSFD) schemes can improve the accuracy and reduce computational costs of traditional finite-difference schemes. However, the development of these schemes is based on analytical solutions and *ad hoc* rules. In this paper, we derive a NSFD scheme based on Green's function formulations for reaction–diffusion–convection systems. The formulation of the NSFD scheme is divided into three stages. In the first one, the domain of the original boundary value problem is decomposed into N subdomains. In the second stage, for each subdomain, integral formulations based on Green's functions are derived for each subdomain. Finally, the resulting integrals are approximated by means of quadrature rules. The proposed NSFD scheme based on Green's function formulation incorporates, in a natural way, the effects of boundary nodes in the discretization approximation (i.e., avoiding the use of heuristic rules), it also exhibits global approximation orders of $O(h^2)$ and leads to smaller approximation errors with respect to standard FD schemes. Numerical simulations on a catalytic particle model and a benchmark tubular reactor model are used for illustrating the accuracy and performance of the proposed NSFD scheme as compared to standard finite differences schemes.

1. Introduction

Systems in which chemical reactions are coupled to diffusion and convection transport arise in different science and engineering fields, including physics, biology, environmental and chemical engineering (Gilding and Kersner, 2004; Murray, 2003). It is well-known that finding analytical solution of nonlinear PDE models is, even if they exist, not a trivial. In this way, approximate numerical solutions have been considered for solving nonlinear PDE (Villadsen and Stewart, 1967; Bayliss et al., 1989; Bermejo and Carpio, 2008; Fatehi et al., 2009). Particularly, several methods have been reported for the numerical solution of reaction–diffusion–convection (RDC) systems (Roos et al., 2008). For example, Alhumaizi et al. (2003) presented a numerical analysis of RDC systems using finite difference, orthogonal collocation, and finite element methods. Coimbra et al. (2004) developed a moving finite element method to solve time dependent RDC problems. Hernandez-Martinez et al. (2011b) derived an integral formulation approach based on Green's function for the numerical solution of a class of RDC systems with Danckwerts-type boundary conditions. Given their properties in stability, efficiency and simplicity of computational implementation (Hildebrand, 1968; Smith, 1985), finite difference (FD) methods have been widely used to solve problems modeled with RDC-PDE. However, it is well-known that the discretization of the differential operators is highly sensitive to round-off errors, which is

* Corresponding author. Tel.: +52 55 58044650; fax +52 55 58044900.
E-mail address: elijazfan@yahoo.com (E. Hernandez-Martinez).

0009-2509/$ - see front matter © 2013 Elsevier Ltd. All rights reserved.
http://dx.doi.org/10.1016/j.ces.2013.03.001

sometimes compensated by the usage of adaptive mesh refinement schemes. In addition, the incorporation of additional parameters in the discretization of continuous systems (e.g., mesh size, integration step) can lead to numerical instabilities.

Oriented to improve the accuracy of FD schemes, Mickens (1989) developed nonstandard finite difference (NSFD) schemes. These schemes can be seen as a generalization of the FD approximation of derivative terms where the step size is replaced by a function that depends on the step size itself and position (Mickens, 1989). This function is obtained by means of the incorporation of analytical solutions and *ad hoc* rules. In addition, the source term can be proposed considering information of the adjacent nodes to the central point (i.e., non-local information). Several results for both partial and ordinary differential equations have shown that such schemes exhibit better performances than traditional FD schemes. Examples of application of NSFD include reaction–convection (Mickens, 1989; Anguelov et al., 2003), reaction–diffusion (Anguelov et al., 2005) and reaction–diffusion–convection systems (Kojouharov and Chen, 1999; Mickens, 2000), ecological and epidemiological models (Mickens, 2007), oscillator models (Mickens, 1994, 1999), among others. A general review of NSFD methods can be found in Patidar (2005). The main drawback of NSFD schemes is that, in general, they are supported on heuristic rules, thus motivating the development of systematic methodologies for their derivation.

Recent works have shown that local and nonlocal NSFD for reaction–diffusion systems can be systematically obtained without the use of Taylor series expansion and heuristic rules. In fact, systematic derivation of NSFD schemes can be based on rigorous Green's function formulations (Alvarez-Ramirez et al., 2007; Hernandez-Martinez et al., 2011a). In addition, the resulting NSFD scheme incorporates weight factors in the discretization of the nodes at the boundaries that improve the numerical approximation of traditional FD schemes (Alvarez-Ramirez et al., 2007). Particularly, in curvilinear coordinate systems (i.e., cylindrical and spherical coordinates), the weight factors describe the curvature effects (Alvarez-Ramirez and Valdes-Parada, 2009), which are not considered in traditional FD schemes.

In this paper, we extend the results of NSFD based on Green's function formulations to dynamical RDC systems with general boundary conditions. This contribution is more general than previous contributions on the use of integral formulation approaches for transport-reaction systems (Alvarez-Ramirez et al., 2007; Alvarez-Ramirez and Valdes-Parada, 2009; Hernandez-Martinez et al., 2011a,b) and highlights the relationship between standard FD and NSFD schemes for a wide class of RDC systems. NSFD based on Green's functions are derived in three stages: (i) The domain of boundary value problem is decomposed into N subdomains. (ii) For each subdomain, an integral approach based on Green's function is formulated. (iii) The resulting integrals are approximated by quadrature rules. General boundary conditions are considered, showing that the NSFD schemes incorporate, in a natural way, the effects of boundary nodes in the discretization approximation. Numerical simulations on a catalytic particle and a benchmark tubular reactor models show that NSFD schemes exhibit both less approximation error and acceptable CPU-time as compared to traditional FD schemes over an important range of physical parameters.

The outline of the paper is as follows. In the following section, a brief description of the Green's function formulation for one-dimensional reaction–diffusion–convection model is derived. In Section 3, classical FD schemes are presented, and then NSFD schemes based on the integral formulation approach are derived. Numerical results on two cases are presented and compared with standard FD schemes in Section 4. Finally, the corresponding conclusions are provided in Section 5.

2. Green's function formulation for a RDC system

In this section, the integral approach based on Green's function is derived for a dimensionless RDC model with general-type boundary conditions.

2.1. Reaction–diffusion–convection one dimensional model

The general PDE under consideration can be described as follows:

$$\frac{\partial u(x,t)}{\partial t} = \frac{\partial^2 u(x,t)}{\partial x^2} - Pe\frac{\partial u(x,t)}{\partial x} - R(u(x,t)), \quad x \in [a,b] \tag{1}$$

with initial condition

$$u(0,x) = u_0(x) \tag{2}$$

and general-type boundary conditions,

$$\alpha_a \frac{\partial u(a,t)}{\partial x} + \beta_a u(a,t) + \gamma_a = 0$$
$$\alpha_b \frac{\partial u(b,t)}{\partial x} + \beta_b u(b,t) + \gamma_b = 0 \tag{3}$$

where α_i, β_i and γ_i, $i = a,b$ are constant parameters; Pe is the Péclet number, which denotes the relationship between the convective and diffusive transport. Eq. (1) with initial (2) and boundary conditions (3) constitute a complete set of equations for the RDC system, which can describe a wide class of distributed parameter systems in engineering. For instance, tubular reactors, contaminant transport problems, interactions of ecological populations, crystallization units, transport phenomena in catalytic particles, etc. (Finlayson, 2006).

2.2. Integral formulation approach based on Green's function

In order to derive the integral formulation for Eq. (1), we follow the development described by Hernandez-Martinez et al. (2011b). Therefore, using the integration factor $\sigma = \exp(-Pex)$, where Pe is constant, we obtain the self-adjoint form of Eq. (1) as

$$\frac{\partial}{\partial x}\left[\exp(-Pex)\frac{\partial u(x,t)}{\partial x}\right] = \exp(-Pex)\Psi(x,t) \tag{4}$$

where $\Psi(x,t) = (\partial u(x,t)/\partial t) + R(u(x,t))$. Let us define

$$L = \frac{\partial}{\partial x}\left[\exp(-Pex)\frac{\partial}{\partial x}\right]$$

in Eq. (4) as the differential operator and introduce Green's function $G(z,x)$. Then, integration by parts of Eq. (4) leads to

$$\int_a^b \frac{G(z,x)}{\exp(Pez)}\Psi(x,t)\,dz = \exp(-Pez)\left[G(z,x)\frac{\partial u(z,t)}{\partial z} - \frac{\partial G(z,x)}{\partial z}u(z,t)\right]_a^b + \int_a^b u(z,t)L^*G(z,x)\,dz \tag{5}$$

On the other hand, the boundary-value problem for $G(z,x)$ is given by

$$L^*G(z,x) = \delta(z-x) \tag{6}$$

with the corresponding homogeneous boundary conditions

$$\alpha_a \frac{\partial G(a,x)}{\partial x} + \beta_a G(a,x) = 0$$
$$\alpha_b \frac{\partial G(b,x)}{\partial x} + \beta_b G(b,x) = 0 \tag{7}$$

where $\delta(z-x)$ is the Dirac delta function. The filtration property of Dirac delta function leads to $\int_a^b u(z,t)\delta(z-x)dz = u(x,t)$ (Greenberg, 1971; Haberman, 2003). After using this property and evaluating the boundary conditions given by Eq. (7), the

following can be obtained:

$$u(x,t)=\exp(-Pea)\frac{\partial G(a,x)}{\partial z}\frac{\gamma_a}{\beta_a}-\exp(-Peb)\frac{\partial G(b,x)}{\partial z}\frac{\gamma_b}{\beta_b}+\int_a^b\frac{G(z,x)}{\exp(Pez)}\Psi(z,t)\,dz \tag{8}$$

Eq. (8) is the integral formulation for Eq. (1) and its solution requires the corresponding Green's function, $G(z,x)$.

2.2.1. Computation of the Green's function

The integration of Eq. (6) with boundary conditions given by Eq. (7), leads to

$$G(z,x)=\frac{1}{Pe}\begin{cases}C_1\left[\exp(Pez)-\exp(Pea)\left(1+\frac{\alpha_a}{\beta_a}Pe\right)\right] & \text{if } z<x\\ C_3\left[\exp(Pez)-\exp(Peb)\left(1+\frac{\alpha_b}{\beta_b}Pe\right)\right] & \text{if } z\geq x\end{cases} \tag{9}$$

The computation of the constants C_1 and C_3 requires imposing two additional conditions. The first condition arises from the fact that the profile $u(x,t)$ is continuous at $z=x$, i.e., $G(x^+,x)=G(x^-,x)$, and the second condition results from the integration of Eq. (6) within the limits $z=x^-$ and $z=x^+$, giving to the following equalities:

$$\left.\frac{\partial G(z,x)}{\partial z}\right|_{z=x^+}-\left.\frac{\partial G(z,x)}{\partial z}\right|_{z=x^-}=\exp(Pex)$$

Evaluating these conditions in Eq. (9) leads to

$$G(z,x)=\frac{1}{G^*}\begin{cases}[\exp(Pez)-\exp(Pea)k_a][\exp(Pex)-\exp(Peb)k_b] & \text{if } z<x\\ [\exp(Pez)-\exp(Peb)k_b][\exp(Pex)-\exp(Pea)k_a] & \text{if } z\geq x\end{cases} \tag{10}$$

where $G^*=Pe[\exp(Peb)k_b-\exp(Pea)k_a]$, $k_a=1+(\alpha_a/\beta_a)Pe$ and $k_b=1+(\alpha_b/\beta_b)Pe$. Eq. (10) is the general Green's function, which as a whole with Eq. (8) denote the integral formulation for RDC-PDE given by Eq. (1). According to the parameters α_i, β_i and γ_i, it is possible to obtain Green's function for different types of boundary conditions (e.g., Dirichlet, Neumman, Robin).

3. Numerical schemes

In this section, we describe the derivation of NSFD schemes based on Green's function formulations. The structure of the proposed NSFD scheme is also discussed. Classical finite difference schemes are described briefly for completeness.

3.1. Classical finite difference schemes

In traditional FD schemes, the spatial operators of RDC model given by Eq. (1) can be discretized in different ways. For instance, for an equidistant grid $X_{N+1}=x_a,x_1,\ldots,x_N,x_b$, where $x_a=a$ and $x_b=b$, with $x_i-x_{i-1}=h$ and $u_i(t)=u(x_i,t)$, one can obtain the semi-discrete form of Eq. (1) as

$$\frac{du_i(t)}{dt}=\frac{(1+\frac{1}{2}Peh)u_{i-1}(t)-2u_i(t)+(1-\frac{1}{2}Peh)u_{i+1}(t)}{h^2}-R(u_i(t)) \tag{11}$$

where $i=1,2,\ldots,N$. The spatial operators (first and second derivative) are approximated by central second-order finite difference (CFD) schemes. For the convective operator, it is also possible to use backward or forward approximations for obtaining the following schemes:

- Forward finite difference (FFD) scheme

$$\frac{du_i(t)}{dt}=\frac{u_{i-1}(t)-(2-Peh)2u_i(t)+(1-Peh)u_{i+1}(t)}{h^2}-R(u_i(t)) \tag{12}$$

- Backward finite difference (BFD) scheme

$$\frac{du_i(t)}{dt}=\frac{(1+Peh)u_{i-1}(t)-(2+Peh)u_i(t)+u_{i+1}(t)}{h^2}-R(u_i(t)) \tag{13}$$

To complete the spatial discretization, it is necessary to introduce the boundary conditions. Ghost nodes and extended grids are typically used in the discretization of boundary conditions of PDE systems by standard FD methods (Hildebrand, 1968; Smith, 1985). Although these formulations can be easily implemented, they assume regularity in the domain, which in some physical situations cannot be well justified. This assumption can lead to weak numerical schemes exhibiting unphysical behaviors. Therefore, with the purpose of avoiding ghost nodes in the derivatives of boundary conditions, discretizations based on first-order FD schemes are commonly used.

3.2. NSFD based on Green's function formulation

For the derivation of NSFD based on Green's function formulation of Eqs. (1)–(3), we follow the development presented in Alvarez-Ramirez et al. (2007). For an equidistant grid, we consider a partially overlapping domain decomposition $D_i=[x_{i-1},x_{i+1}]$, $i=1,\ldots,N$. Then, we obtain the following set of differential equations:

$$\begin{aligned}&Lu(x,t)=\Psi(x,t),\quad x\in D_1,\quad \alpha_a\frac{\partial u(x_a,t)}{\partial x}+\beta_a u(x_a,t)+\gamma_a=0\quad\text{and}\\ &u(x_2,t)=u_2(t)\\ &Lu(x,t)=\Psi(x,t),\quad x\in D_i,\quad u(x_{i-1},t)=u_{i-1}(t)\quad\text{and}\\ &u(x_{i+1},t)=u_{i+1}(t),\quad i=2,\ldots,N-1\\ &Lu(x,t)=\Psi(x,t),\quad x\in D_N,\quad u(x_{N-1},t)=u_{N-1}(t)\quad\text{and}\\ &\alpha_b\frac{\partial u(x_b,t)}{\partial x}+\beta_b u(x_b,t)+\gamma_b=0\end{aligned} \tag{14}$$

To illustrate the procedure, we consider Eqs. (14) with Dirichlet-type boundary conditions (i.e., $x\in D_i$). Then, in accordance with the results of Section 2, the integral formulation for Eqs. (14) is

$$u(x,t)=\exp(Pex_{i-1})\frac{\partial G_i(x_{i-1},x)}{\partial z}u_{i-1}(t)-\exp(Pex_{i+1})\frac{\partial G_i(x_{i+1},x)}{\partial z}u_{i+1}(t)+\int_{x_{i-1}}^{x_{i+1}}\frac{G_i(z,x)}{\exp(Pez)}\Psi(z,t)\,dz \tag{15}$$

and considering Dirichlet-type boundary conditions ($\alpha_a=\alpha_a=0$ and $\beta_a=\beta_b=1$) in Eq. (10), the corresponding Green's functions are

$$G_i(z,x)=\frac{1}{G^*}\begin{cases}[\exp(Pex)-\exp(Pex_{i+1})][\exp(Pez)-\exp(Pex_{i-1})] & \text{if } z<x\\ [\exp(Pez)-\exp(Pex_{i+1})][\exp(Pex)-\exp(Pex_{i-1})] & \text{if } z\geq x\end{cases} \tag{16}$$

where $G^*=Pe[\exp(Pex_{i+1})-\exp(Pex_{i-1})]$. The evaluation of Eq. (15) at the interior point x_i for each subdomain D_i yields

$$u_i(t)=-\frac{[\exp(Pex_i)-\exp(Pex_{i-1})]}{\exp(Pex_{i+1})-\exp(Pex_{i-1})}u_{i+1}(t)-\frac{[\exp(Pex_{i+1})-\exp(Pex_i)]}{\exp(Pex_{i+1})-\exp(Pex_{i-1})}u_{i-1}(t)+\int_{x_{i-1}}^{x_{i+1}}\frac{G_i(z,x)}{\exp(Pez)}\Psi(z,t)\,dz \tag{17}$$

In order to approximate the integrals in Eq. (17), the trapezoidal rule for three equidistant points is used. This leads to the following expression:

$$\int_{x_{i-1}}^{x_{i+1}}\frac{G_i(z,x)}{\exp(Pez)}\Psi(z,t)\,dz$$

$$\approx -\frac{[\exp(Pex_i)-\exp(Pex_{i-1})][\exp(Pex_{i+1})-\exp(Pex_i)]}{Peh\exp(Pex_i)[\exp(Pex_{i+1})-\exp(Pex_{i-1})]}h^2\Psi_i(t) \tag{18}$$

Substituting Eqs. (18) into (17):

$$\begin{aligned}u_i(t) = &-\frac{[\exp(Pex_i)-\exp(Pex_{i-1})]}{\exp(Pex_{i+1})-\exp(Pex_{i-1})}u_{i+1}(t)\\ &-\frac{[\exp(Pex_{i+1})-\exp(Pex_i)]}{\exp(Pex_{i+1})-\exp(Pex_{i-1})}u_{i-1}(t)\\ &-\frac{[\exp(Pex_i)-\exp(Pex_{i-1})][\exp(Pex_{i+1})-\exp(Pex_i)]}{Peh\exp(Pex_i)[\exp(Pex_{i+1})-\exp(Pex_{i-1})]}h^2\Psi_i(t)\end{aligned}$$

or

$$a_iu_{i-1}(t)-b_iu_i(t)+c_iu_{i+1}(t)=\Psi_i(t) \tag{19}$$

Repeating the procedure described in Eq. (15) to Eq. (19) for the subdomains D_1 and D_N, we obtain the following set of equations:

$$\begin{aligned}\frac{du_1(t)}{dt} &= a_1\frac{\gamma_a}{\beta_a}-b_1u_1(t)+c_1u_2(t)-R(u_1(t))\\ \frac{du_i(t)}{dt} &= a_iu_{i-1}(t)-b_iu_i(t)+c_iu_{i+1}(t)-R(u_i(t))\\ \frac{du_N(t)}{dt} &= a_Nu_{N-1}(t)-b_Nu_N(t)+c_N\frac{\gamma_b}{\beta_b}-R(u_N(t))\end{aligned} \tag{20}$$

with the discretization parameters

$$\begin{aligned}a_1 &= \frac{Pe\xi_1}{h(C_1\xi_a-\xi_1)},\quad b_1=\frac{\xi_2-\xi_ak_a}{\xi_1-\xi_2}a_1,\quad c_1=\frac{\xi_1-\xi_ak_a}{\xi_2-\xi_1}a_1\\ a_i &= \frac{Pe\xi_i}{h(\xi_i-\xi_{i-1})},\quad b_i=\frac{\xi_{i+1}-\xi_{i-1}}{\xi_{i+1}-\xi_i}a_i,\quad c_i=\frac{Pe\xi_i}{h(\xi_{i+1}-\xi_i)}\\ a_N &= \frac{\xi_N-\xi_bk_b}{\xi_N-\xi_{N-1}}c_N,\quad b_N=\frac{\xi_{N-1}-\xi_bk_b}{\xi_N-\xi_{N-1}}c_N,\quad c_N=\frac{Pe\xi_N}{h(\xi_N-C_2\xi_b)}\end{aligned}$$

where $\xi_i=\exp(Pex_i)$, $C_1=1+\frac{3}{2}(\alpha_a/\beta_a)Pe$ and $C_2=1+\frac{3}{2}(\alpha_b/\beta_b)Pe$.

Some comments regarding the structure of NSFD based on Green's function formulations derived above are in order:

- The weight parameters a_i, b_i and c_i, $i=1,\ldots,N$ are functions of h. According to definition by Mickens (1989), the system given by Eq. (20) can be regarded as a NSFD scheme for RDC systems with general-type boundary conditions.
- Traditionally, NSFD schemes for reaction-transport PDE are derived using the subequation method (Mickens, 2000; Anguelov et al., 2005). The resulting subequations are discretized using exact FD and heuristic rules. Finally, the discrete equations are assembled. In the development described above, we have shown that the NSFD for RDC models can be obtained by Green's function formulations without the use of empiric rules, i.e., the a_i, b_i and c_i parameters arise only by Green's function properties.
- The standard FD scheme given by Eqs. (11) is a particular case of NSFD based on Green's function formulation. To prove this, in Eq. (20) the a_i parameter is multiplied by $\xi_{i-1/2}/\xi_{i-1/2}$, obtaining

$$a_i=\frac{Pe\exp(\frac{1}{2}Peh)}{h(\exp(\frac{1}{2}Peh)-\exp(-\frac{1}{2}Peh))}$$

Considering the first two terms of the Taylor expansion of the exponential function, it results that $a_i\approx(1+\frac{1}{2}Peh)/h^2$. Then, using ξ_i/ξ_i and $\xi_{i+1/2}/\xi_{i+1/2}$ for the b_i and c_i, respectively, we obtain that $b_i\approx 2/h^2$ and $c_i\approx(1-\frac{1}{2}Peh)/h^2$. In this form, it is possible to recover the central finite difference scheme given by Eqs. (11).

- The set of equations in (20) is a NSFD scheme for general (one-dimensional) reaction–transport problems. In this case, it is possible to obtain particular cases for reaction–diffusion or diffusion–convection. For instance, if we consider $Pe\to 0$ (i.e., convective transport is not important in the global process), the weight parameters of Eq. (20) are

$$\begin{aligned}a_1 &= \frac{h}{h^2\left(h-\frac{3}{2}\frac{\alpha_a}{\beta_a}\right)},\quad b_1=\frac{2h-\frac{\alpha_a}{\beta_a}}{h^2\left(h-\frac{3}{2}\frac{\alpha_a}{\beta_a}\right)},\quad c_1=\frac{h-\frac{\alpha_a}{\beta_a}}{h^2\left(h-\frac{3}{2}\frac{\alpha_a}{\beta_a}\right)},\\ a_i &= \frac{1}{h^2},b_i=\frac{2}{h^2},c_i=\frac{1}{h^2},\\ a_N &= \frac{h-\frac{\alpha_b}{\beta_b}}{h^2\left(h+\frac{3}{2}\frac{\alpha_b}{\beta_b}\right)},\quad b_N=\frac{2h-\frac{\alpha_b}{\beta_b}}{h^2\left(h+\frac{3}{2}\frac{\alpha_b}{\beta_b}\right)},\quad c_N=-\frac{h}{h^2\left(h+\frac{3}{2}\frac{\alpha_b}{\beta_b}\right)},\end{aligned}$$

obtaining the NSFD for a reaction–diffusion system with general-type boundary conditions. Notice that, for Dirichlet-type boundary conditions, a_i, b_i and c_i coincide with the classical FD scheme. If we consider mixed-type boundary conditions ($\partial u(0,t)/\partial t$ and $u(1,t)=1$), the weight parameters at the boundaries are $b_1=c_1=\frac{2}{3}$, $a_1=c_N=0$, $a_N=1$ and $b_N=2$. This result was found by Alvarez-Ramirez et al. (2007), where extensive numerical simulations showed that the weight 3/2 has an important effect on the performance of the FD scheme by reducing the approximation error about 10% for coarse grids. Notice that the weight factor 3/2 arises from the implementation of the boundary parameters (a_1 and c_N). This indicates that the proposed numerical scheme will exhibit better performance than classical FD under different-type boundary conditions.
- The use of the trapezoidal rule for the integral discretization introduces the factor 3/2, which leads to a second-order NSFD scheme. The use of a rectangle rule (first-order numerical integration) removes the factor 3/2 leading to a first-order approximation in the boundary nodes. This implies an approximation order of $O(h)$. By considering a higher order integration (i.e., Simpson's rule), it is possible to obtain NSFD schemes with higher approximation orders.
- Although, for simplicity in presentation, the analysis was developed for one-dimensional RDC systems, the NSFD development can be extended to two or three dimensions. For example, consider a two dimensional RDC model as follows:

$$\frac{\partial u(x,y,t)}{\partial t}=\frac{\partial^2u(x,y,t)}{\partial x^2}+\frac{\partial^2u(x,y,t)}{\partial y^2}-Pe_x\frac{\partial u(x,y,t)}{\partial x}-R(u(x,y,t)) \tag{21}$$

A direct way to obtain the NSFD scheme is by means of the separate treatment of the spatial differential operators. After regrouping Eq. (21) it is possible to obtain Eq. (4) and repeating the steps given by Eqs. (14)–(20)), one can obtain the following set of equations:

$$\begin{aligned}\frac{\partial u_1(y,t)}{\partial t}-\frac{\partial^2u_1(y,t)}{\partial y^2} &= a_1\frac{\gamma_a}{\beta_a}-b_1u_1(y,t)+c_1u_2(y,t)-R(u_1(y,t))\\ \frac{\partial u_i(y,t)}{\partial t}-\frac{\partial^2u_i(y,t)}{\partial y^2} &= a_iu_{i-1}(y,t)-b_iu_i(y,t)+c_iu_{i+1}(y,t)-R(u_i(y,t))\\ \frac{\partial u_N(y,t)}{\partial t}-\frac{\partial^2u_N(y,t)}{\partial y^2} &= a_Nu_{N-1}(y,t)-b_Nu_N(y,t)+c_N\frac{\gamma_b}{\beta_b}-R(u_N(y,t))\end{aligned} \tag{22}$$

Finally, the procedure is repeated for each equation in the system (22), leading to a system of ODEs. Another option is the determination of the integral formulation for the

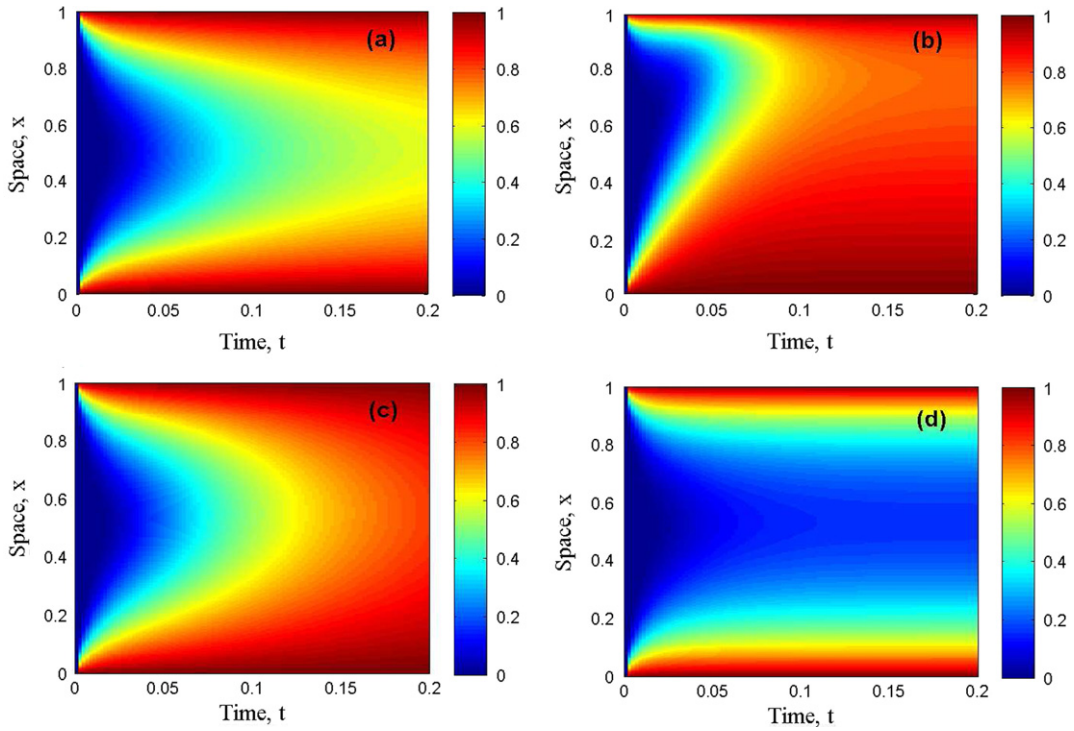

Fig. 1. Spatio-temporal profiles for the catalytic particle model for different values of Pe and ϕ. (a) $\phi=2.0$ and $Pe=0.1$; (b) $\phi=2.0$ and $Pe=10$; (c) $\phi=0.5$ and $Pe=1.0$; (d) $\phi=5.0$ and $Pe=1.0$.

two-dimensional model, Eq. (21), with subsequent application of the trapezoidal rule for the surface or volume integral.

- The derivation of the NSFD scheme considers Robin-type boundary conditions. NSFD schemes for RDC systems with boundary conditions that depend on the history of the reaction (i.e., nonlocal boundary conditions) can be obtained in a similar way. For the internal nodes $(2,\ldots,N-1)$ the procedure is the same, while that the α, β and γ parameters of the nodes 1 and N will depend of the nonlocality in the boundary conditions.

4. Numerical results

This section presents the ability of NSFD scheme based on Green's functions to produce an accurate solution for reaction–diffusion–convection models described by Eq. (1). To this end, we consider two cases: (i) a RDC problem in a catalytic particle and (ii) nonisothermal chemical tubular reactor. To evaluate the performance of the proposed numerical scheme, steady-state and dynamical simulations were analyzed and compared with a classical FD scheme. For the steady-state case, the discrete form of the spatial operators was obtained and the nonlinear set of algebraic equations was solved by Newton–Raphson algorithms. For the dynamical case, we used the method of lines (MOL), where we obtained a set of semi-discrete equations by the spatial discretization and the set of ordinary differential equations was integrated in time using Runge–Kutta routines (Logist et al., 2009). All numerical simulations were performed on a PC with AMD Turion (tm) II P560 processor Dual-Core with 4.0 GB in RAM memory. In order to present a fair comparison with a high degree of accuracy, the numerical results obtained with the NSDF and FD were compared with the analytic solution for the catalytic particle example, and numerical solution obtained with COMSOL Multiphysics 4.3a using 2000 nodes for the tubular reactor example.

4.1. Catalytic particle

Consider Eq. (1) with a linear function $R(u(x))=\phi^2u(x,t)$, which can describe the reaction–diffusion–convection problem in a catalytic particle (Coimbra et al., 2004). Then, the mathematical model is given by

$$\frac{\partial u(x,t)}{\partial t}=\frac{\partial^2u(x,t)}{\partial x^2}-Pe\frac{\partial u(x,t)}{\partial x}-\phi^2u(x) \tag{23}$$

with initial and boundary conditions as $u(x,0)=0$, $u(0,t)=1$ and $u(1,t)=1$, respectively. The function $u(x,t)$ corresponds to the normalized concentration; ϕ is Thiele modulus, which relates chemical reaction rate and the diffusive transport; the dimensionless parameters $x\in[0,1]$ and $t>0$ denote the spatial coordinate and time, respectively. To illustrate the effects of chemical reaction and transport phenomena in the dynamic of the catalytic particle, Fig. 1 shows the spatio-temporal simulations for different values of Pe and ϕ.

4.1.1. Steady-state case

Consider Eq. (23) with $\partial u(x,t)/\partial t=0$, one can obtain the analytic solution as

$$u(x)=\frac{\exp(m_2x)[\exp(m_1)-1]+\exp(m_1x)[1-\exp(m_2)]}{\exp(m_1)-\exp(m_2)} \tag{24}$$

where

$$m_1=\frac{\sqrt{Pe^2+4\phi^2}}{2},\quad m_2=\frac{\sqrt{Pe^2-4\phi^2}}{2}$$

As a single index for measuring approximation errors, we have calculated the maximum error (E_m), defined as

$$E_m=\max\left|\frac{u_e(x_i)-u(x_i)}{u_e(x_i)}\right| \tag{25}$$

where $u_e(x_i)$ and $u(x_i)$ are related to the analytic solution and the approximate solution evaluated at the point x_i, respectively. For

the numerical simulations, we used backward, forward and central FD schemes given by Eqs. (11)–(13) and the NSFD scheme described in Eq. (20) with $\alpha_a=\alpha_b=0$, $\beta_a=\beta_b=1$ and $\gamma_a=\gamma_b=-1$. The set of algebraic equations was solved using Newton–Raphson subroutine from Matlab package.

For different values of Pe and ϕ, Fig. 2 shows the E_m as a function of number of nodes N. To appreciate the effect of convective transport over the performance of the proposed numerical scheme, we consider $\phi=2$ and four values of Pe (0.1, 1.0, 10 and 100). When the diffusive transport dominates over convective effects ($Pe<1$), Fig. 2 shows that same maximum errors of NSFD and CFD can be observed. For the case when convective transport is more important than diffusive transport ($Pe<1$), the NSFD presents lower E_m than all FD schemes. Particularly, for $Pe=100$ CFD scheme shows 3 order of magnitude higher than NSFD. This result indicates that the proposed numerical scheme can reduce the numerical approximation errors that arise in processes where the global process is dominated by convective transport. On the other hand, for a constant value of Pe, the effects of the chemical reaction on the performance of numerical scheme, can be observed. Fig. 3 shows that NSFD scheme provides smaller approximation errors than the classical FD schemes. This outperforming is more important for small values of ϕ, since NSFD scheme is based on the analytic inversion of the differential operator that is related with diffusive and convective processes.

Figs. 2 and 3 indicate that, in general, NSFD and CFD schemes show approximation order of $O(h^2)$, while FFD and BFD exhibit only $O(h)$. This is because the global approximation orders of classical FD schemes depend on the convective operator approximation, i.e., if the convective operator is approximated with first-order FD, the global order is reduced to first-order. On the other hand, in the derivation of the NSFD scheme it is not necessary the approximation of the convective operator. Indeed, Green's function formulation leads, in a natural form, to a global second-order approximation.

4.1.2. Dynamical case

For this case, to obtain a reference solution of the catalytic particle model the Laplace transform was applied to Eq. (23). In this case, the analytical solution was found using the Laplace transform method and it is given by Eq. (24) with $m_1=\sqrt{Pe^2+4(s+\phi^2)}/2$ and $m_2=\sqrt{Pe^2-4(s+\phi^2)}/2$. Unfortunately, the inverse Laplace transform for this expression is not available. In order to determinate the solution in the time-domain, we used the numerical inversion by Zakian's algorithm (Zakian, 1975; Taiwo et al., 1995). To quantify the approximation errors, we consider the temporal maximum error (E_t) defined as

$$E_t=\sum_{k}^{N}\max\left|\frac{u_e(x_i,t_k)-u(x_i,t_k)}{u_e(x_i,t_k)}\right| \tag{26}$$

where N is the total number of time step (final time/δt), $u(x_i,t_k)$ is an approximation of the concentration profile at time $k\delta t$ and $u_e(x_i,t_k)$ is the computed value of concentration profile via numerical inversion Laplace transform using tolerances of 10^{-10}.

For $N=50$ and different values of Pe and ϕ, Fig. 4 shows the concentration profiles and their respective E_t. As expected, for a wide range of Pe and ϕ better agreements between the reference solution and NSFD approximations are observed. This is in line

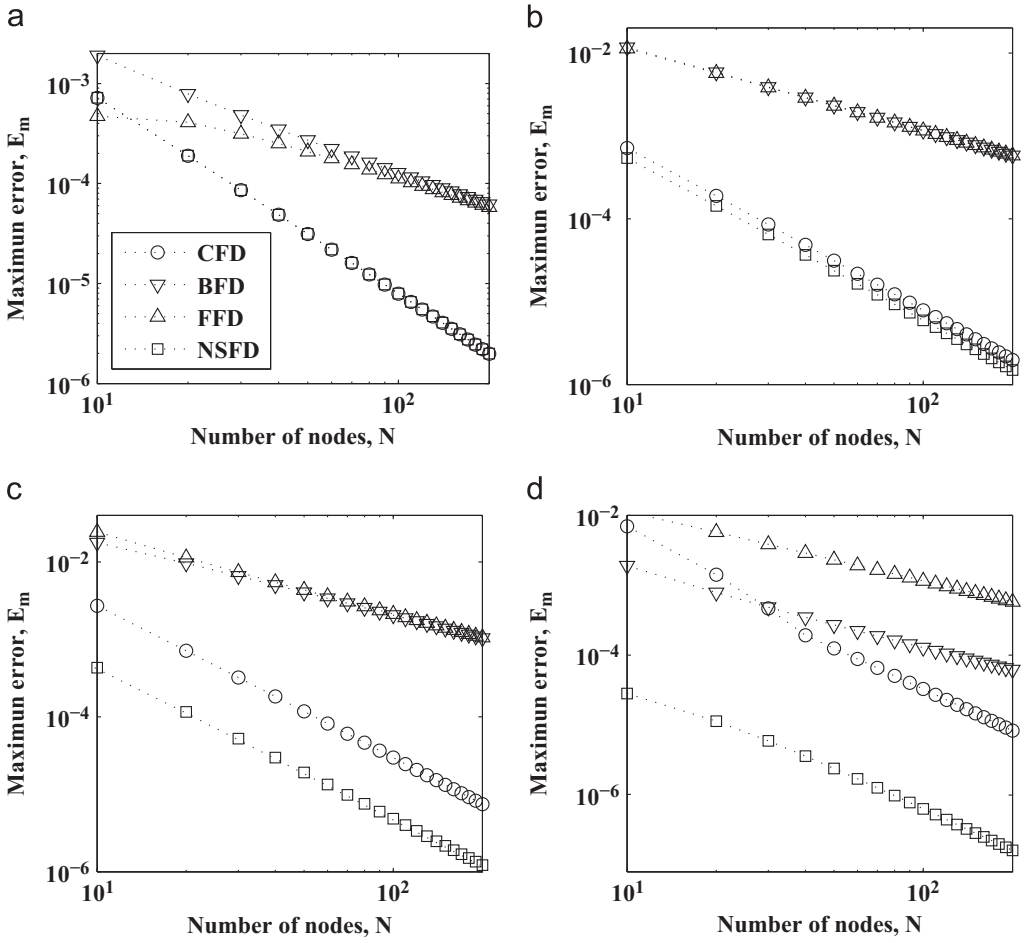

Fig. 2. Maximum error (E_m) as a function of the number of nodes (N), for $\phi=2.0$ and (a) $Pe=0.1$, (b) $Pe=1.0$, (c) $Pe=10$ and (d) $Pe=100$.

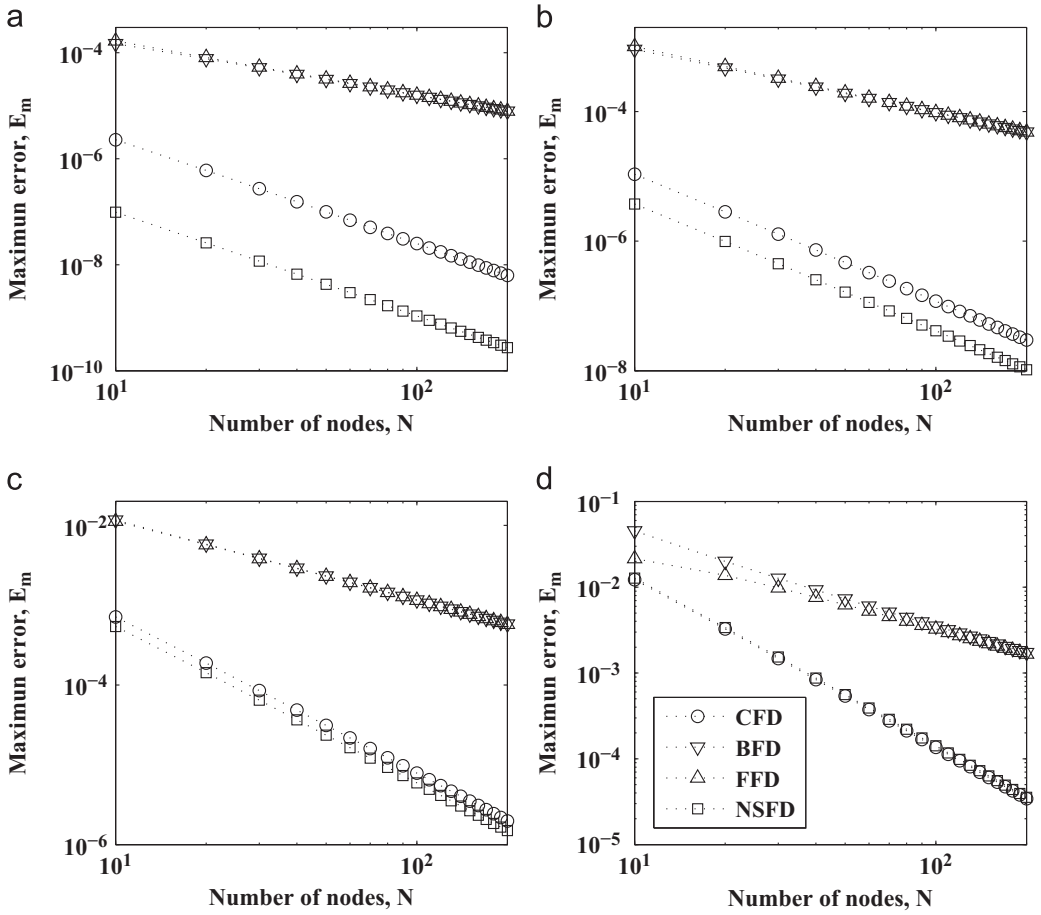

Fig. 3. Maximum error (E_m) as a function of the number of nodes (N), for $Pe=1.0$ and (a) $\phi=0.1$, (b) $\phi=0.5$, (c) $\phi=1.0$ and (d) $\phi=5.0$.

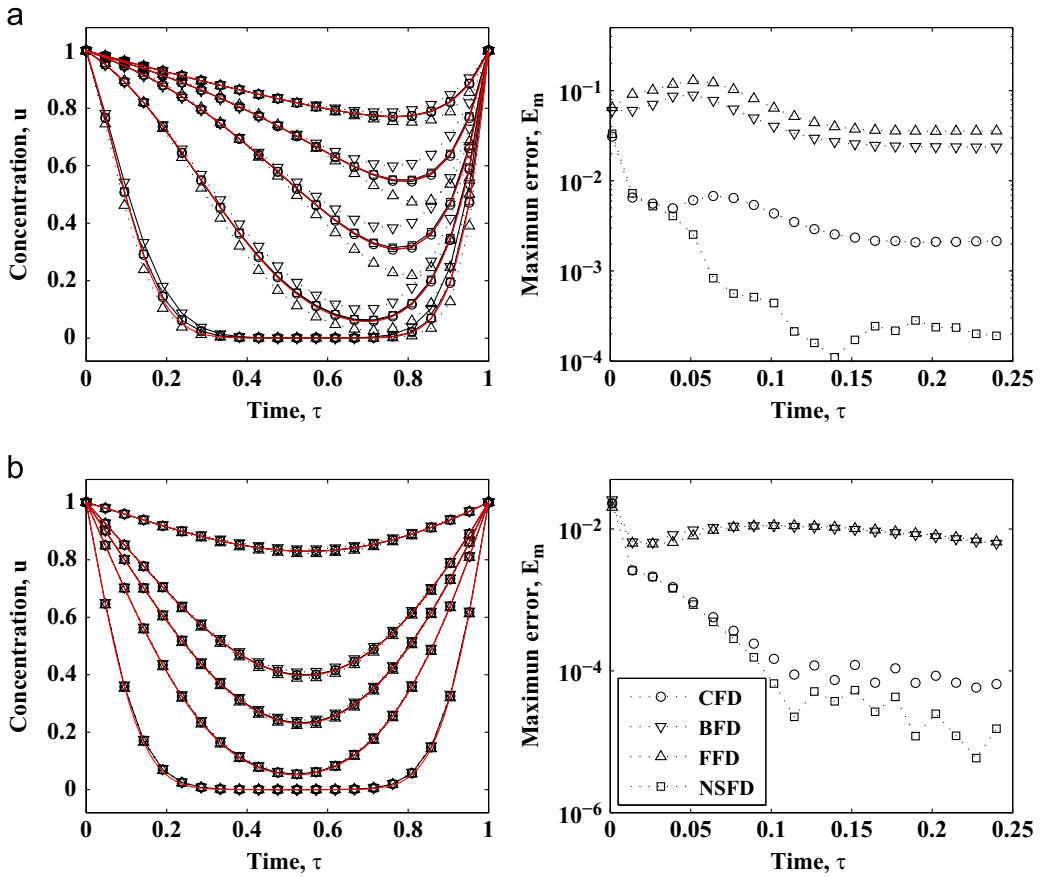

Fig. 4. Concentration profiles at different times and their respective E_t, (a) $Pe=10$ and $\phi=2.0$; (b) $Pe=1.0$ and $\phi=0.1$.

with the E_t values since, for example, for convection dominant conditions the NSFD exhibits approximation errors about two order of magnitudes smaller than CFD scheme.

4.2. Tubular reactor with axial dispersion

As a second example, we consider an axial dispersion tubular reactor model. The mass and energy balance equations are two coupled nonlinear parabolic PDEs, which in dimensionless form are given as (Jensen and Ray, 1982)

$$\frac{\partial y(\xi,t)}{\partial t} = \frac{1}{Pe_y}\frac{\partial^2 y(\xi,t)}{\partial \xi^2} - \frac{\partial y}{\partial \xi} + BDa(1-z(\xi,t))\exp\left(\frac{y(\xi,t)}{1-y(\xi,t)/\lambda}\right) - \sigma(y(\xi,t)-y_j) \quad (27)$$

Table 1
Set of parameters for different behaviors of the tubular chemical reactor: (a) quasi-linear, (b) hot spot and (c) periodic oscillations dynamics.

Parameter	(a)	(b)	(c)
Pe_y	5.0	5.0	5.0
Pe_z	5.0	5.0	5.0
λ	20.0	20.0	20.0
B	11.0	5.0	14.0
Da	0.174	0.875	0.185
σ	2.25	5.0	3.0
y_j	0.1	0.1	0.0

$$\frac{\partial z(\xi,t)}{\partial t} = \frac{1}{Pe_z}\frac{\partial^2 z(\xi,t)}{\partial \xi^2} - \frac{\partial z}{\partial \xi} + BDa(1-z(\xi,t))\exp\left(\frac{y(\xi,t)}{1-y(\xi,t)/\lambda}\right) \quad (28)$$

with boundary conditions:

$$\left.\frac{\partial y(\xi,t)}{\partial \xi}\right|_{\xi=0} = Pe_y y(t,0) \quad \left.\frac{\partial z(\xi,t)}{\partial \xi}\right|_{\xi=0} = Pe_z y(t,0)$$

$$\left.\frac{\partial y(\xi,t)}{\partial \xi}\right|_{\xi=1} = 0 \quad \left.\frac{\partial z(\xi,t)}{\partial \xi}\right|_{\xi=1} = 0$$

and initial conditions

$$y(\xi,0)=0, \quad z(\xi,0)=0$$

where $y(\xi,t)$ and $z(\xi,t)$ are dimensionless temperature and concentration, respectively. Da is the Damköhler. Pe_y and Pe_z are the Péclet numbers for mass and heat transfer. σ is a dimensionless heat transfer coefficient, B is a dimensionless adiabatic temperature rise and λ is a dimensionless activation energy. Depending of the values of the model parameters, the temperature profiles can exhibit different behaviors, such as quasi-linear, hot spot or stable periodic oscillations. Table 1 presents the set of parameters and Fig. 5 shows the spatio-temporal profiles corresponding to these behaviors. For the numerical analysis, we have focused on the influence of physical parameters as Damköhler and Péclet numbers. That is, when Da is large, the process is dominated by the reaction and when Da is small the process is dominated by the transport phenomena. On the other hand, if $Pe \to 0$ the transport is dominated by diffusion and if $Pe \to \infty$ the transport is dominated by convection.

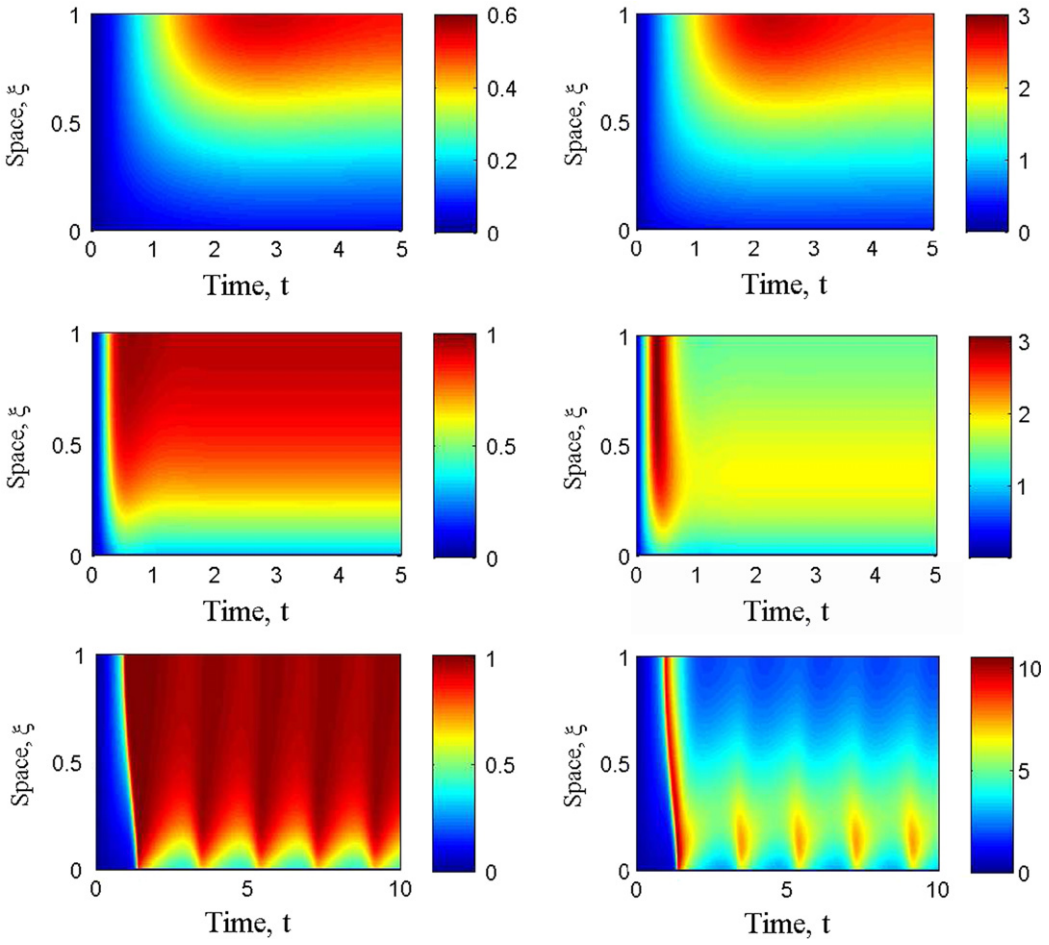

Fig. 5. Spatio-temporal profiles of concentration and temperature of the tubular reactor, (a) cuasi-linear, (b) hot-spot and (c) periodic oscillatory dynamics.

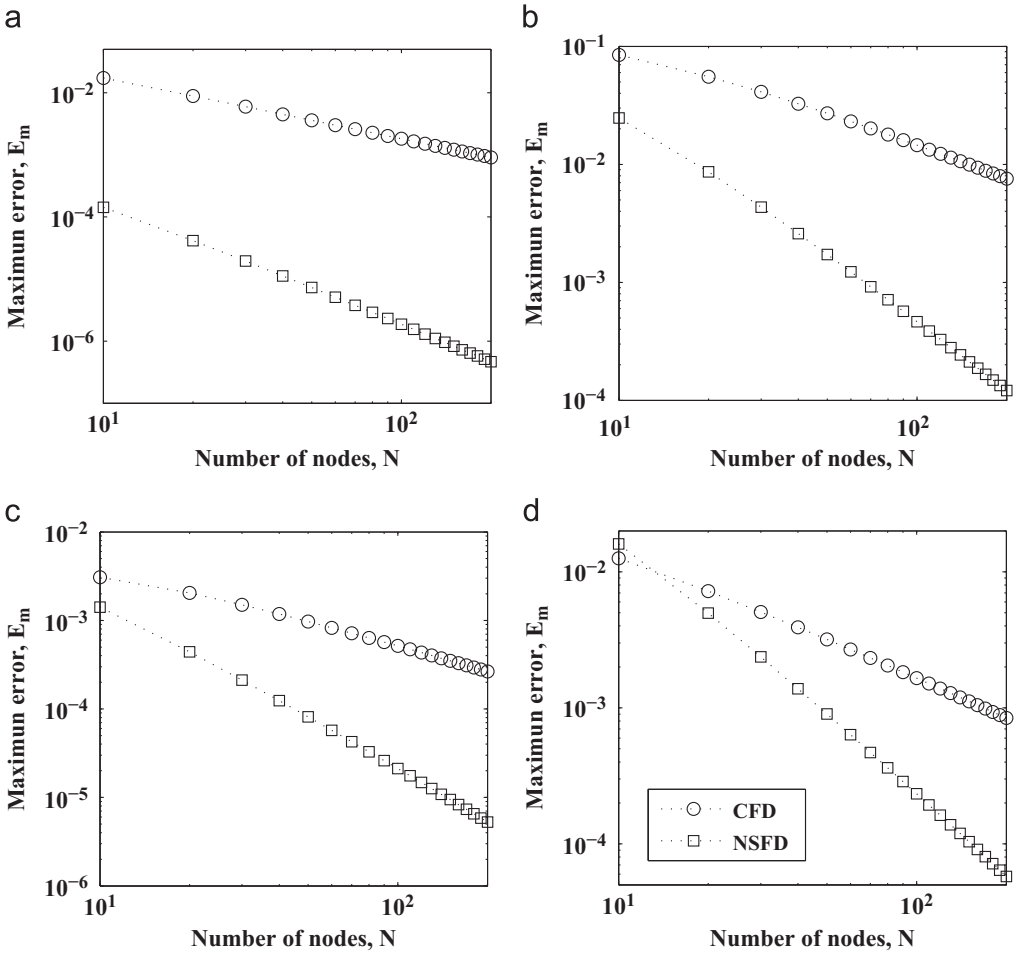

Fig. 6. Steady-state profiles of the tubular chemical reactor. Maximum error vs number of nodes for (a) $Pe=0.1$ and $Da=0.875$, (b) $Pe=10$ and $Da=0.875$; (c) $Pe=5.0$ and $Da=0.5$; (d) $Pe=5.0$ and $Da=5.0$.

Table 2
CPU-time (sec) for the steady-state solution of the tubular reactor model, (a) $Da=0.875$ and (b) $Pe=1.0$.

(a)			(b)		
Pe	NSFD	CFD	*Da*	NSFD	CFD
0.01	14.352	12.729	0.01	8.408	7.347
0.05	14.008	11.746	0.05	7.051	7.815
0.1	13.603	11.715	0.1	10.795	7.971
0.5	13.854	11.512	0.5	12.495	10.436
1.0	14.118	11.965	1.0	16.146	12.963
5.0	15.865	13.135	5.0	56.846	48.235
10.0	15.631	12.745	10.0	23.150	19.681
50.0	16.161	12.776	50.0	155.002	140.68
100.0	17.113	13.228	100.0	121.896	107.749

4.2.1. NSFD scheme based on Green's function

Unlike Eq. (1) where the Péclet number is multiplying the convection operator, in the tubular reactor model the inverse of Péclet numbers are multiplying to the diffusion and convection operators. For simplicity in the development, we consider $Pe_y = Pe_z = Pe$. Then, the self-adjoint operator is $L = \frac{\partial}{\partial x}[(\exp(-Pex)/Pe)(\partial/\partial x)]$. Therefore, the integral formulation and Green's function are

$$u(x,t) = \frac{\exp(-Pea)}{Pe}\frac{\partial G(a,x)}{\partial z}\frac{\gamma_a}{\beta_a} - \frac{\exp(-Peb)}{Pe}\frac{\partial G(b,x)}{\partial z}\frac{\gamma_b}{\beta_b} + \int_a^b \frac{G(z,x)}{\exp(Pez)}\Psi(z,t)\,dz \tag{29}$$

$$G(z,x) = \frac{1}{G^*}\begin{cases} [\exp(Pez)-\exp(Pea)k_a][\exp(Pex)-\exp(Peb)k_b] & \text{if } z<x \\ [\exp(Pez)-\exp(Peb)k_b][\exp(Pex)-\exp(Pea)k_a] & \text{if } z\geq x \end{cases} \tag{30}$$

where $G^* = [\exp(Peb)k_b - \exp(Pea)k_a]$. Following the procedure presented in Eqs. (14)–(19), it is not hard to show that the NSFD scheme is given by

$$\begin{aligned} \frac{du_1(t)}{dt} &= \frac{a_1\frac{\gamma_a}{\beta_a} - b_1u_1(t) + c_1u_2(t)}{Pe} - R(u_1(t)) \\ \frac{du_i(t)}{dt} &= \frac{a_iu_{i-1}(t) - b_iu_i(t) + c_iu_{i+1}(t)}{Pe} - R(u_i(t)) \\ \frac{du_N(t)}{dt} &= \frac{a_Nu_{N-1}(t) - b_Nu_N(t) + c_N\frac{\gamma_b}{\beta_b}}{Pe} - R(u_N(t)) \end{aligned} \tag{31}$$

where the parameters a_i, b_i and c_i are described in Eqs. (20).

4.2.2. Steady-state case

Consider Eqs. (27) and (28) under steady-state conditions, i.e. $\partial y/\partial t = 0$ and $\partial z/\partial t = 0$. The maximum error is calculated by Eq. (25). In order to appreciate the effect of the physical phenomena (i.e., transport phenomena and reaction rate) in the numerical predictions, we show the maximum errors for different values of *Pe* and *Da*.

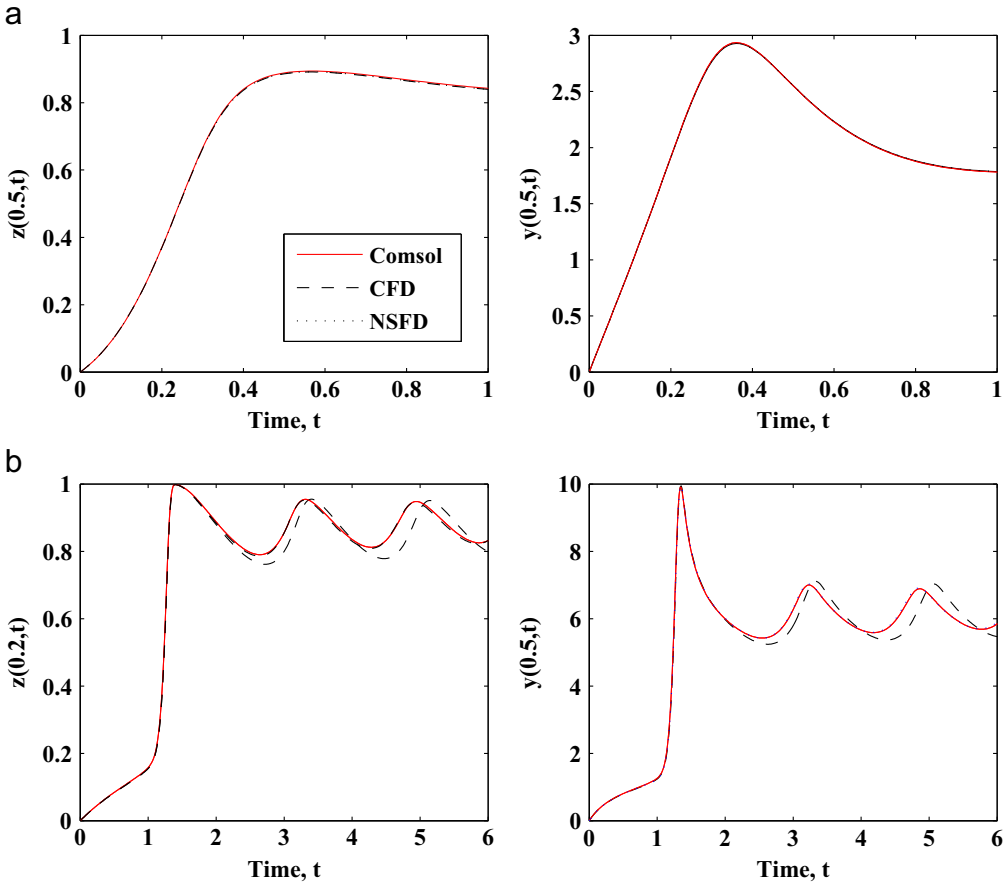

Fig. 7. Dynamic profiles of the tubular chemical reactor, (a) temperature profiles with hot spot and (b) temperature and concentration profiles with periodic oscillations.

Table 3
CPU-time (sec) for the dynamical solution of the tubular reactor model, (a) $Da=0.875$ and (b) $Pe=1.0$.

(a)			(b)		
Pe	NSFD	CFD	*Da*	NSFD	CFD
0.01	4.867	5.569	0.01	8.985	9.937
0.05	4.098	4.149	0.05	9.212	10.077
0.1	4.823	4.960	0.1	9.469	9.656
0.5	7.597	7.488	0.5	9.204	9.764
1.0	9.219	9.734	1.0	9.110	9.845
5.0	10.670	13.946	5.0	9.469	9.672
10.0	6.271	6.286	10.0	9.500	9.687
50.0	6.011	6.443	50.0	9.342	9.078
100.0	5.112	5.148	100.0	9.893	10.322

Consider the set of parameters corresponding to hot spot behavior (Table 1). Fig. 6 shows that NSFD scheme performs better numerical approximations than CFD scheme. Given the mathematical structure of tubular reactor model ($1/Pe$ multiplying the diffusive operator), the best performance of NSFD is observed when the global process is dominated by diffusion phenomena. Although the numerical approximation of NSFD is diminished for high Pe values, $O(h^2)$ in the numerical approximations is maintained, while the classical FD schemes the usage of first order approximations in the derivative of boundary conditions leads to numerical approximations of $O(h)$.

On the other hand, the CPU-time required for the numerical solution of the tubular reactor model to different conditions is shown in Table 2. The CPU-time is calculated as the average time needed to obtain the profile $u(x)$ for 10–200 nodes with a spacing of 10 nodes. To observe the effects of both the reactive and transport phenomena on the CPU-time, we proposed to vary the Damköhler and Péclet numbers. In general, Table 2 indicates that the traditional central FD scheme exhibits slightly better computation times than NSFD. That is, since the α, β and γ parameters are functions of exponential functions, these functions require more time to calculate. Nevertheless, NSFD exhibits acceptable CPU-time and the approximation order is maintained in $O(h^2)$.

4.2.3. Dynamical case

In this case, the numerical solution with 2000 nodes obtained from the COMSOL package is considered as reference solution. For the numerical simulations, we used the MOL method with a 4/5-order Runge-Kutta method (ode45 from Matlab Package) and $\delta t=0.01$ for the integration of the differential equations. The tubular reactor with periodic oscillations and hot spot dynamics are considered. In order to compare the performance of NSFD based on Green's function, Fig. 7 shows the temperature and concentration profiles using $N=100$, where it is possible to observe that for hot spot dynamic, both methods present an adequate agreement with the reference solution. However, for periodic oscillations behavior, NSFD scheme shows better correspondence with the COMSOL solution than CFD. This result suggests that NSFD based on integral formulations is a good alternative for the numerical solution of models with complex spatio-temporal patterns. To evaluate the CPU-time, we consider $N=200$ and $t=50$ for different Da and Pe values. For this case, the NSFD scheme exhibits less CPU-time than CFD (Table 3). This suggests that the proposed methodology is a good alternative to solving RDC systems.

5. Conclusions

In this work, we have presented a nonstandard finite differences scheme based on Green's function formulations for numerical solution of nonlinear RDC systems with general-type boundary conditions. It was shown that by using this approach, weighted factors are incorporated in a natural way, leading to NSFD schemes of accuracy $O(h^2)$ even at the boundary nodes without resorting to heuristic rules (e.g., ghost nodes). Overall, Green's function formulation becomes a common framework to back up both traditional and nonstandard FD schemes without making use of Taylor expansions. In this way, the proposed approach can be extended for more generals schemes (e.g., nonlocal schemes). For the numerical accuracy evaluation of NSFD, our results were compared with the standard FD scheme for a wide range of value parameters, finding that the NSFD offers better numerical performance.

References

Alhumaizi, K., Henda, R., Soliman, M., 2003. Numerical analysis of a reaction–diffusion–convection system. Comput. Chem. Eng. 27, 579–594.

Alvarez-Ramirez, J., Valdes-Parada, F.J., Alvarez, J., Ochoa-Tapia, J.A., 2007. A Green's function formulation for finite-differences schemes. Chem. Eng. Sci. 62, 3083–3091.

Alvarez-Ramirez, J., Valdes-Parada, F.J., 2009. Non-standard finite-differences schemes for generalized reaction–diffusion equations. J. Comput. Appl. Math. 228, 334–343.

Anguelov, R., Lubuma, J.M., Mahudu, S.K., 2003. Qualitatively stable finite difference schemes for advection-reaction equations. J. Comput. Appl. Math. 158, 19–30.

Anguelov, R., Kama, R., Lubuma, J.M., 2005. On nonstandard finite difference models of reaction–diffusion equations. J. Comput. Appl. Math. 175, 11–29.

Bayliss, A., Gottlieb, D., Matkowsky, B.J., Minkoff, M., 1989. An adaptive pseudo-spectral method for reaction diffusion problems. J. Comp. Phys. 81, 421–443.

Bermejo, R., Carpio, J., 2008. An adaptive finite element semi-Lagrangian implicit-explicit Runge–Kutta–Chebyshev method for convection dominated reaction–diffusion problems. Appl. Numer. Math. 58, 16–39.

Coimbra, M., Sereno, C., Rodrigues, A., 2004. Moving finite element method: applications to science and engineering problems. Comput. Chem. Eng. 28, 597–603.

Fatehi, R., Manzari, M.T., Hannani, S.K., 2009. A finite-volume ELLAM for non-linear flux convection–diffusion problems. Int. J. Non-Linear Mech. 44, 130–137.

Finlayson, B.A., 2006. Introduction to Chemical Engineering Computing. John Wiley & Sons, New Jersey.

Greenberg, M.D., 1971. Applications of Green's Functions in Science and Engineering. Prentice Hall, New York.

Gilding, B.H., Kersner, R., 2004. Travelling Waves in Nonlinear Diffusion Convection Reaction. Birkhauser.

Haberman, R., 2003. Applied Partial Differential Equations with Fourier Series and Boundary Value Problems. Prentice Hall, New York.

Hernandez-Martinez, E., Valdes-Parada, F.J., Alvarez-Ramirez, J., 2011a. A green's function formulation of nonlocal finite-differences schemes for reaction–diffusion equations. J. Comput. Appl. Math. 235, 3096–3103.

Hernandez-Martinez, E., Alvarez-Ramirez, J., Valdes-Parada, F.J., Puebla, H., 2011b. An integral formulation approach for numerical solution of tubular reactors models. Int. J. Chem. React. Eng. 9, S12.

Hildebrand, F., 1968. Finite-Difference Equations and Simulations. Prentice-Hall, New York.

Jensen, K., Ray, W., 1982. The bifurcation behavior of tubular reactors. Chem. Eng. Sci. 37, 199–222.

Kojouharov, H.V., Chen, B.M., 1999. Non-standard methods for the convective transport equation with nonlinear reactions. Numer. Meth. Part. D. E. 15, 617–624.

Logist, F., Saucez, P., Van-Impe, J., Vande-Wouwer, A., 2009. Simulation of (bio)chemical processes with distributed parameters using matlab. Chem. Eng. J. 155, 603–616.

Mickens, R.E., 1989. Exact solution to a finite difference model of a nonlinear reaction-advection equation: implications for numerical analysis. Numer. Meth. Part. D. E. 5, 313–325.

Mickens, R.E., 1994. Nonstandard Finite Difference Models of Differential Equations. World Scientific, Singapore.

Mickens, R.E., 1999. Discretizations of nonlinear differential equations using explicit nonstandard methods. J. Comput. Appl. Math. 110, 181–185.

Mickens, R.E., 2000. Applications of Nonstandard Finite Difference Schemes. World Scientific, Singapore.

Mickens, R.E., 2007. Calculation of denominator functions for nonstandard finite difference schemes for differential equations satisfying a positivity condition. Numer. Meth. Part. D. E. 23, 672–691.

Murray, J.D., 2003. Mathematical Biology. Springer, New York.

Patidar, K.C., 2005. On the use of nonstandard finite difference methods. J. Differential Equation Appl. 11, 735–758.

Roos, H., Stynes, M., Tobiska, L., 2008. Robust numerical methods for singularly perturbed differential equations: convection–diffusion–reaction and flow problems. Springer Series in Computational Mathematics, vol. 24.

Smith, G.D., 1985. Numerical Solution of Partial Differential Equations: Finite Difference Methods. Oxford University Press, Oxford.

Taiwo, O., Schultz, J., Krebs, V., 1995. A comparison of two methods for the numerical inversion of Laplace transform. Comput. Chem. Eng. 19, 303–305.

Villadsen, J., Stewart, W.E., 1967. Solution of boundary-value problems by orthogonal collocation. Chem. Eng. Sci. 22, 1483–1501.

Zakian, V., 1975. Properties of IMN and JMN approximates and applications to numerical inversion of Laplace transforms and initial value problems. J. Math. Anal. Appl. 50, 191–222.